
**SOLID-STATE
SPECTROSCOPY**

Luminescence of Excitons and Antisite Defects in $\text{Lu}_3\text{Al}_5\text{O}_{12}:\text{Ce}$ Single Crystals and Single-Crystal Films

Yu. V. Zorenko*, V. I. Gorbenko*, G. B. Stryganyuk*, V. N. Kolobanov**,
D. A. Spasskii**, K. Blazek***, and M. Nikl****

* Franko Lviv National University, Lviv, 79017 Ukraine

** Moscow State University, Moscow, 119899 Russia

*** Crytur Ltd., 51101 Turnov, Czech Republic

**** Institute of Physics, AS CZ, 16253 Prague, Czech Republic

Received August 4, 2004

Abstract—The luminescence of excitons and antisite defects (ADs) was investigated, as well as the specific features of the excitation energy transfer from excitons and ADs to the activator (Ce^{3+} ion) in phosphors based on $\text{Lu}_3\text{Al}_5\text{O}_{12}:\text{Ce}$ (LuAG:Ce) single crystals and single-crystalline films, which are characterized by significantly different concentrations of ADs of the $\text{Lu}_{\text{Al}}^{3+}$ type and vacancy-type defects. The luminescence band with $\lambda_{\text{max}} = 249$ nm in LuAG:Ce single-crystal films is due to the luminescence of self-trapped excitons (STEs) at regular sites of the garnet lattice. The excited state of STEs is characterized by the presence of two radiative levels with significantly different transition probabilities, which is responsible for the presence of two excitation bands with $\lambda_{\text{max}} = 160$ and 167 nm and two components (fast and slow) in the decay kinetics of the STE luminescence. In LuAG:Ce single crystals, in contrast to single-crystal films, the radiative relaxation of STEs in the band with $\lambda_{\text{max}} = 253.5$ nm occurs predominantly near $\text{Lu}_{\text{Al}}^{3+}$ ADs. The intrinsic luminescence of LuAG:Ce single crystals at 300 K in the band with $\lambda_{\text{max}} = 325$ nm ($\tau = 540$ ns), which is excited in the band with $\lambda_{\text{max}} = 175$ nm, is due to the radiative recombination of electrons with holes localized near $\text{Lu}_{\text{Al}}^{3+}$ ADs. In LuAG:Ce single crystals, the excitation of the luminescence of Ce^{3+} ions occurs to a large extent with the participation of ADs. As a result, slow components are present in the luminescence decay of Ce^{3+} ions in LuAG:Ce single crystals due to both the reabsorption of the UV AD luminescence in the $4f-5d$ absorption band of Ce^{3+} ions with $\lambda_{\text{max}} = 340$ nm and the intermediate localization of charge carriers at ADs and vacancy-type defects. In contrast to single crystals, in phosphors based on LuAG:Ce single-crystal films, the contribution of slow components to the luminescence of Ce^{3+} ions is significantly smaller due to a low concentration of these types of defects. © 2005 Pleiades Publishing, Inc.

INTRODUCTION

Cerium-activated lutetium aluminum garnet, $\text{Lu}_3\text{Al}_5\text{O}_{12}:\text{Ce}$ (LuAG:Ce), is one of the most effective fast scintillators [1, 2]. In comparison with $\text{Y}_3\text{Al}_5\text{O}_{12}:\text{Ce}$ (YAG:Ce), the closest well-studied analogue, LuAG:Ce single crystals and single-crystal films are characterized by a much larger absorption coefficient of ionizing radiation [3, 4], and their light yields amount to 0.6 and 0.86 of those of YAG:Ce single crystals and single-crystal films [2, 5, 6]. In this context, LuAG:Ce single-crystal films are also used as screens for visualization of x-ray images [2–5].

At the same time, garnet single crystals and single-crystal films are characterized by significantly different concentrations of substitutional and vacancy-type defects [7, 8]. Such differences in the concentrations of these defects in single crystals and single-crystal films are caused by the differences in the methods and mechanisms of crystallization of single crystals from melt

and single-crystal films from flux, the growth temperatures (1800–1900 and 900–1050°C for single crystals and single-crystal films, respectively), and the compositions of the gaseous media used (generally, Ar or vacuum for single crystals and air for single-crystal films). In particular, in $\text{A}_3\text{Al}_5\text{O}_{12}$ ($A = \text{Y}, \text{Lu}$) garnet single crystals, the concentration of specific substitutional defects—antisite defects (ADs) of the $\text{Y}_{\text{Al}}^{3+}$ and $\text{Lu}_{\text{Al}}^{3+}$ types—is 0.05–0.1 formula units (0.25–0.5 at %) [9], whereas single-crystal films of these garnets are free of ADs [10]. In this context, garnet single crystals and single-crystal films can also serve as convenient model objects for studying the regularities of radiative decay of low-energy excitations (especially, the exciton luminescence) in phosphors based on complex multisublattice oxides with garnet [7, 8] or perovskite [11] structures.

We showed in previous studies [8, 10, 12] that ADs are analogues of cationic isoelectronic impurities. Hence, they form radiative recombination centers

responsible for the intrinsic UV luminescence of garnet single crystals at room temperature. In the case of single-crystal garnet films of the same composition, the concentration of luminescence centers related to ADs or vacancy-type defects is extremely low [10, 13]. This circumstance makes it possible to study the exciton luminescence in a given garnet by the example of a single-crystal film of this compound excluding the luminescence of centers related to these types of defects.

In this paper, we report the results of studying the luminescence of excitons and ADs in LuAG:Ce single crystals and single-crystal films, as well as the specific features of the excitation energy transfer to the activator (Ce^{3+} ions).

SAMPLES AND EXPERIMENTAL METHODS

A comparative investigation of the luminescence of LuAG:Ce single crystals and single-crystal films was performed at 9 and 300 K upon excitation by synchrotron radiation with energies of 3–25 eV of the DORIS III positron storage ring at HASYLAB, DESY (Hamburg, Germany). The use of synchrotron radiation with an energy near the fundamental absorption edge and interband transitions in garnets, where the absorption coefficient generally ranges from 10^4 to $2 \times 10^5 \text{ cm}^{-1}$ [8], makes it possible to compare the luminescence characteristics of single crystals with those of single-crystal films even several micrometers thick since, in the latter case, synchrotron radiation with an energy of 5–10 eV is totally absorbed in a single-crystal film. The measurement system makes it possible to record the luminescence spectra and the excitation luminescence spectra both in the integration mode and with a time delay with respect to the 0.127-ns pulse of exciting synchrotron radiation. In particular, the luminescence and the luminescence excitation spectra were recorded in the time intervals 0–50 and 150–200 ns within a repetition period of synchrotron radiation pulses (200 ns).

The luminescence decay kinetics was measured in the time interval 0–200 ns at 9 and 300 K using a photomultiplier in the integration mode.

LuAG:Ce single crystals were obtained at Crytur Ltd. (Turnov, Czech Republic) by the Czochralski method in molybdenum crucibles in a reduction atmosphere from a charge containing background impurities with a concentration less than or equal to 10–100 ppm. Single-crystal films were grown from a melt solution based on the $\text{PbO-B}_2\text{O}_3$ flux by liquid phase epitaxy on undoped garnet (YAG) substrates at the Laboratory of Optoelectronic Materials (Lviv University). The raw material was of the same class of purity. No additional doping was used to eliminate the significant (0.093 Å) lattice mismatch between the LuAG:Ce single-crystal films and the single-crystal YAG substrate.

The concentration of Ce^{3+} ions in the single crystals and the single-crystal films was close to 0.05 formula units (0.25 at %).

RESULTS AND DISCUSSION

The luminescence spectra of LuAG:Ce single crystals and single-crystal films upon excitation by synchrotron radiation with energies in the region of interband transitions at 10.77 eV (115 nm) (curve 1), near the fundamental absorption edge at 7.74 eV (160 nm) (curve 2), and in the region of intracenter $4f-5d$ transitions in Ce^{3+} ions at 5.5 eV (225 nm) (curve 3) are shown in Figs. 1 (9 K) and 2 (300 K). In the visible spectral range, the luminescence of LuAG:Ce single crystals and single-crystal films is caused by the transitions from the lower term $5d^1$ of the t_{2g} shell to the ${}^2F_{5/2, 7/2}$ levels of the ground state of the f shell of Ce^{3+} ions. The two-component structure of this emission band ($\lambda_{\text{max}} = 498$ and 550 nm) is well-resolved in the case of low-temperature (9 K) measurements (Fig. 1, curves 3).

The luminescence spectrum of LuAG single crystals in the UV range at 9 K (Fig. 1a) upon excitation by synchrotron radiation with an energy exceeding the band gap (curve 1) is a nonelementary emission band that is a superposition of two bands: a strong one with $\lambda_{\text{max}} = 253.5$ nm (4.89 eV) and a band an order of magnitude weaker with $\lambda_{\text{max}} = 320$ nm (3.87 eV). The first luminescence band is due to the self-trapped exciton (STE) luminescence [8], whereas the spectral position of the second band is close to that of the luminescence band due to the centers formed by $\text{Lu}_{\text{Al}}^{3+}$ ADs [8, 13]. Upon excitation of LuAG:Ce single crystals near the fundamental absorption edge ($E = 7.8$ eV), the intensity of the STE luminescence in the band at 253.5 nm increases significantly (Fig. 1a, curve 2).

In contrast to LuAG single crystals, upon excitation of LuAG:Ce single-crystal films in the region of interband transitions ($E = 17.2$ eV), UV luminescence is completely absent (Fig. 1b, curve 1). At the same time, upon excitation by synchrotron radiation with an energy of 7.3 eV near the fundamental absorption edge in LuAG:Ce single-crystal films, STE luminescence is observed in the band at 249 nm (4.97 eV) (Fig. 1b, curve 2), which is asymmetrically extended to lower energies. We should note two important specific features of the STE luminescence in LuAG:Ce single-crystal films: (i) its intensity in the band at 4.97 eV is significantly (by an order of magnitude) lower (Fig. 1b, curve 2) than under the same excitation conditions for the corresponding single crystals (Fig. 1a, curve 2) and (ii) the STE luminescence maximum (at 4.89 eV) in single crystals is significantly shifted to lower energies with respect to the corresponding maximum at 4.97 eV in LuAG:Ce single-crystal films. These specific features of the STE luminescence are due to the significant

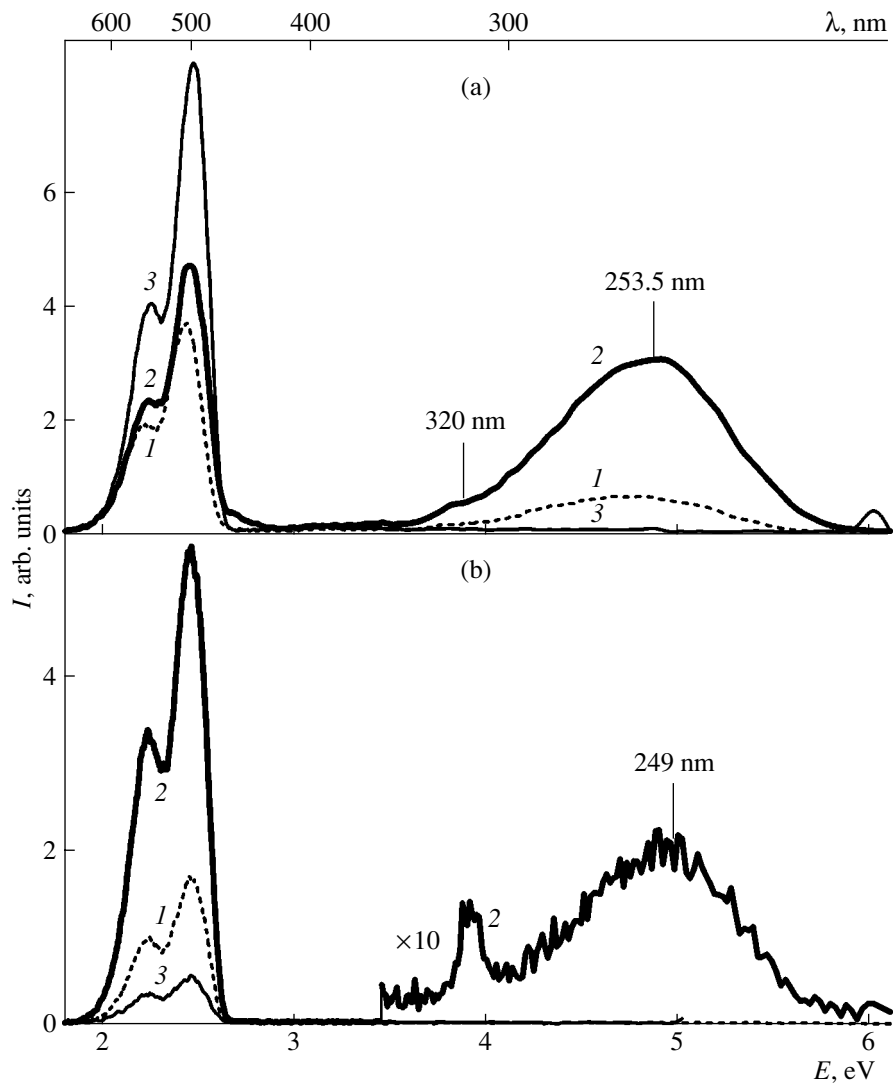


Fig. 1. Luminescence spectra of (a) LuAG:Ce single crystals and (b) LuAG:Ce single-crystal films at 9 K upon excitation by synchrotron radiation with energies of (1 (b)) 17.2, (1 (a)) 10.8, (2 (a)) 7.8, (2 (b)) 7.3, and (3) 5.4 eV.

differences in the AD concentrations in LuAG:Ce single crystals and single-crystal films.

With an increase in temperature from 9 to 300 K, the STE luminescence is quenched in LuAG:Ce single crystals. This process is accompanied by the enhancement of the AD luminescence (Fig. 2a, curves 1, 2) in the bands with $\lambda_{\max} = 318$ and 375 nm. The AD luminescence maximum in LuAG:Ce single crystals is reached at 100 K, after which the temperature quenching of the luminescence of $\text{Lu}_{\text{Al}}^{3+}$ ADs occurs. It should be noted that the bands mentioned above do not belong to different centers. Their presence is due to the reabsorption of the wide UV luminescence band of $\text{Lu}_{\text{Al}}^{3+}$ ADs, peaked presumably near 325 nm, by the absorption band with $\lambda_{\max} = 340$ nm, which corresponds to the $4f^7(^2F_{5/2}) \rightarrow 5d^1$ transitions in Ce^{3+} ions. The bands with $\lambda_{\max} = 318$ and 375 nm have excitation spectra and

luminescence decay kinetics of the same type. As in the case of measurements at 9 K (Fig. 1a), upon excitation of LuAG:Ce single crystals at 300 K by synchrotron radiation with an energy in the exciton absorption region, the intensity of the luminescence of $\text{Lu}_{\text{Al}}^{3+}$ ADs increases significantly (Fig. 2a, curve 2).

In contrast to single crystals, single-crystal films show the complete absence of UV AD luminescence at 300 K (Fig. 2b). The low-intensity luminescence bands peaked at 313 nm (3.95 eV) and 387 nm (3.20 eV) (Fig. 2a, curves 1 and 2, respectively) observed upon excitation of LuAG:Ce single-crystal films by synchrotron radiation with energies of 11.1 eV (the region of interband transitions) and 7.3 eV (the region of exciton absorption) are due to the background impurities of Gd^{3+} and Pb^{2+} ions, respectively (flux components in the case of flux crystallization of single-crystal films), rather than to ADs.

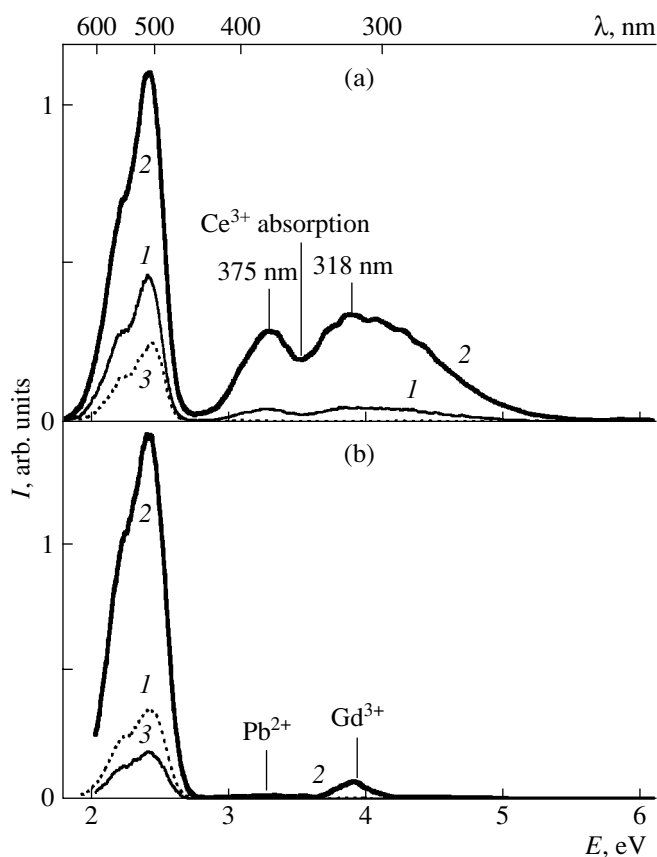


Fig. 2. Luminescence spectra of (a) LuAG:Ce single crystals and (b) LuAG:Ce single-crystal films at 300 K upon excitation by synchrotron radiation with energies of (1) 11.1, (2 (a)) 7.8, (2 (b)) 7.3, and (3) 5.5 eV.

The luminescence excitation spectrum of STEs in LuAG:Ce single-crystal films at 9 K is a nonelementary band located near the LuAG fundamental absorption edge (Fig. 3a, curve 1). The structure of this excitation band (two peaks with $\lambda_{\max} = 160$ and 167 nm) suggests the presence of two excited exciton levels. This structure, in particular, correlates with a certain asymmetry of the STE luminescence spectrum of LuAG:Ce single-crystal films in the long-wavelength spectral region (Fig. 1b, curve 2), which suggests also the presence of two emission bands (by analogy with the σ and π STE luminescence bands in alkali halide crystals [14]).

In comparison with the STE luminescence excitation band of LuAG:Ce single-crystal films, the corresponding excitation band in the spectra of LuAG:Ce single crystals is less structured and is shifted significantly to a shorter wavelength of 170 nm (7.28 eV) (Fig. 3a, curve 2). It is noteworthy that, in the same spectral region, excitation of the luminescence of Lu³⁺ ADs in the bands with $\lambda_{\max} = 318$ and 375 nm occurs at 9 K in a narrow band with $\lambda_{\max} = 172.5$ nm (7.18 eV) on the long-wavelength wing of the fundamental

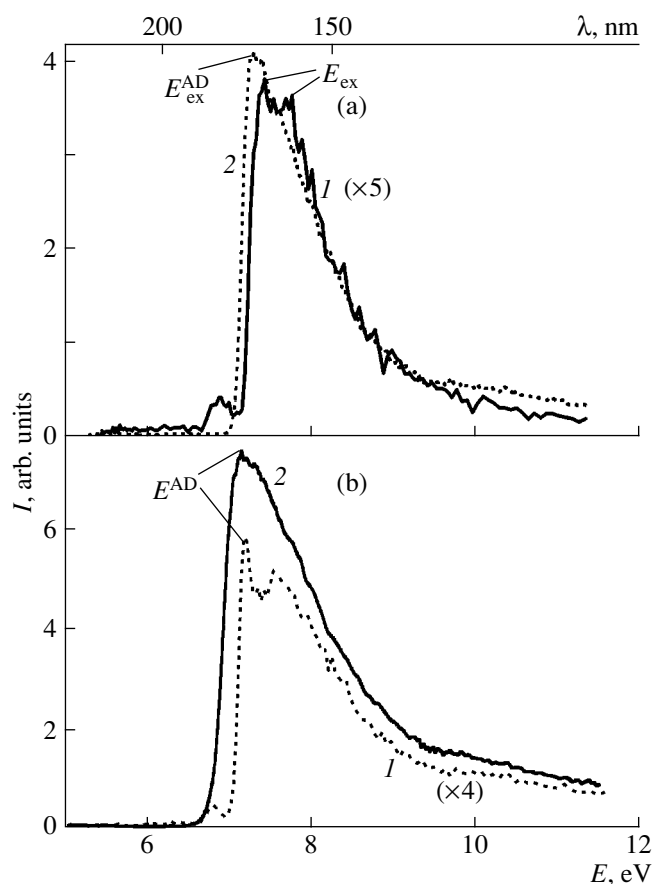


Fig. 3. (a) Luminescence excitation spectra at the wavelength $\lambda = 250$ nm in (1) LuAG:Ce single-crystal films and (2) LuAG:Ce single crystals at 9 K; (b) luminescence excitation spectra of LuAG:Ce single crystals at wavelengths of 295 nm at 9 K (1) and 323 nm at 300 K (2).

absorption edge of LuAG (Fig. 3b, curve 1). With an increase in temperature to 300 K, the peak of the AD luminescence excitation shifts to a longer wavelength at 175 nm (7.07 eV) (Fig. 3b, curve 2).

The intensity of the STE luminescence excitation in LuAG:Ce single crystals is higher than that for single-crystal films by a factor of more than 5 under the same experimental conditions (Fig. 3a). This result is supplemented by the spectral proximity of the STE (170 nm) and AD (172.5 nm) luminescence peaks in the spectra of LuAG:Ce single crystals. These facts indicate that the STE radiative relaxation in LuAG:Ce single crystals occurs predominantly near ADs, which are analogues of isoelectronic cation impurities [8, 10]. In essence, the STE luminescence in single-crystal garnets is the luminescence of bound excitons with a modulated (due to the localization near isoelectronic impurities) energy spectrum. The high AD concentration (up to 0.5 at %) in single crystals is the reason for the high intensity of the STE luminescence in comparison with single-crystal films, where the radiative annihilation of excitons occurs predominantly at regular sites of the garnet lattice.

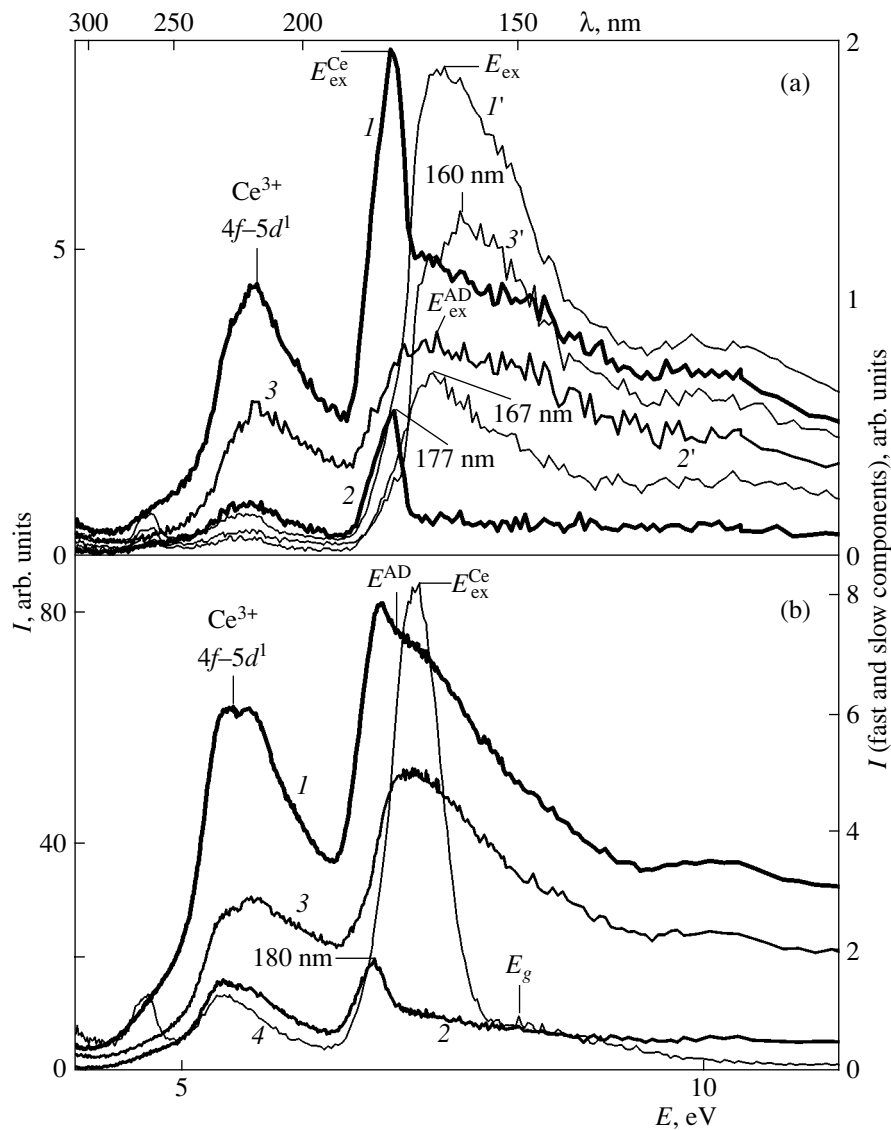


Fig. 4. (a) Luminescence excitation spectra of Ce^{3+} ions in the band with $\lambda_{max} = 515$ nm of LuAG:Ce single crystals at ($I-3$) 9 and ($I'-3'$) 300 K measured in the integrated mode (I) and in the time intervals (2) 0–50 and (3) 150–200 ns after the excitation pulse of synchrotron radiation with a duration of 0.127 ns; (b) luminescence excitation spectra of Ce^{3+} ions in the band with $\lambda_{max} = 515$ nm ($I-3$) measured in the integrated mode (I) and in the time intervals (2) 0–50 and (3) 150–200 ns in comparison with the similar spectra of LuAG:Ce single crystals ($I'-3'$).

The luminescence excitation spectra of Ce^{3+} ions in LuAG:Ce single crystals and single-crystal films are shown in Figs. 4a and 4b, respectively. At 9 K, the fast component of the luminescence of Ce^{3+} ions in LuAG:Ce single crystals is excited predominantly in a narrow peak at $\lambda_{max} = 177$ nm (6.99 eV) (Fig. 4a, curve 2). The shape of this excitation band (a narrow strong line in the exciton absorption region) is indicative of the radiative annihilation of excitons localized near defects or impurities. We believe that the peak at 6.99 eV corresponds to the energy of formation of STEs related to Ce^{3+} ions, with a wave function strongly correlated with the activator [8].

The slow components of the luminescence of Ce^{3+} ions in LuAG:Ce single crystals are excited mainly in the bands with $\lambda_{max} = 170-172$ nm (7.28–7.20 eV) and 150 nm (8.25 eV) (Fig. 4a, curve 3). The first excitation band is close to the corresponding luminescence excitation bands of Y_{Al}^{3+} ADs ($\lambda_{max} = 172$ nm) and AD-related excitons ($\lambda_{max} = 170$ nm). The second excitation band with $\lambda_{max} = 150$ nm corresponds to the energy of the beginning of interband transitions in LuAG [13]. Thus, even at low temperatures, the excitation of the luminescence of Ce^{3+} ions in LuAG:Ce single crystals occurs partially through recombination pro-

cesses at the sites of location of both Ce^{3+} ions and $\text{Lu}_{\text{Al}}^{3+}$ ADs.

With an increase in temperature from 9 to 300 K, the maximum of the fast component of the luminescence of Ce^{3+} ions in LuAG:Ce single crystals shifts to longer wavelengths up to 180 nm (Fig. 4b, curve 2'). At room temperature, the contribution of the slow components of excitation of the luminescence of Ce^{3+} ions increases significantly in the band with $\lambda_{\text{max}} = 175$ nm due to the presence of $\text{Lu}_{\text{Al}}^{3+}$ ADs (Fig. 4b, curves 1, 3). With an increase in temperature to 300 K, the luminescence intensity of Ce^{3+} ions also increases in the band with $\lambda_{\text{max}} = 230$ nm, which is due to the $4f^2(F_{5/2}) \rightarrow 5d^1(2e)$ transitions in Ce^{3+} ions (Fig. 4b, curve 1).

The luminescence excitation spectra of Ce^{3+} ions in LuAG:Ce single-crystal films at 9 K (Fig. 4a, curves 1'–3') differ significantly from the corresponding spectra of LuAG:Ce single crystals (curves 1–3). In the spectra of LuAG:Ce films, the AD-related excitation band near 172.5 nm is completely absent. The maxima of excitation of both the fast ($\lambda = 167$ nm) and the slow ($\lambda = 160$ nm) components of the luminescence of Ce^{3+} ions in the band at 2.4 eV (515 nm) in LuAG:Ce single-crystal films (Fig. 4a, curves 1', 2') almost coincide with the corresponding maxima of excitation of the STE luminescence in LuAG:Ce single-crystal films. This fact indicates the predominantly exciton mechanism of excitation of the luminescence of Ce^{3+} ions in LuAG:Ce single-crystal films. The presence of two maxima in the luminescence excitation spectrum of Ce^{3+} ions in the exciton absorption region shows that, as in the case of STEs at regular garnet lattice sites, the excited state of an exciton localized near Ce^{3+} ions has two radiative levels with different transition probabilities.

At the same time, the excitation spectra of both the fast and the slow luminescence components of Ce^{3+} ions in LuAG:Ce single-crystal films at 9 K also contain a band with $\lambda_{\text{max}} = 150$ nm (8.25 eV) corresponding to the beginning of interband transitions in LuAG (Fig. 4a, curves 2', 3'). This fact indicates that the excitation of the luminescence of Ce^{3+} ions in LuAG:Ce single-crystal films occurs partially through recombination. Since the Ce^{3+} ion is the center of intermediate localization of holes [15], the luminescence is excited due to the recombination of an electron with a hole localized near a Ce^{3+} ion with subsequent excitation energy transfer to Ce^{3+} ions.

With an increase in temperature, the maximum of excitation of the luminescence of Ce^{3+} ions in LuAG:Ce single-crystal films shifts to a shorter wavelength (Fig. 4b, curve 4). At 300 K, the maximum is located at 7.2 eV (172 nm). At the same time, the shape of the excitation curve does not undergo any significant changes. This fact indicates that, in the room temperature range, the dominant mechanism of excitation of the luminescence of Ce^{3+} ions in LuAG:Ce single-crystal

films is the exciton mechanism, in contrast to LuAG:Ce crystals, in which the contribution of the AD-related excitation mechanism is significant. This indication is confirmed convincingly by the study of the decay kinetics of Ce^{3+} ions in LuAG:Ce single crystals and single-crystal films at 9 and 300 K (Figs. 5a, 5b and 6a, 6b, respectively).

Figure 5a shows the luminescence decay kinetics of Ce^{3+} ions in LuAG:Ce single crystals at 9 K upon excitation in the two $4f$ – $5d$ absorption bands of Ce^{3+} ions with $h\nu_{\text{max}} = 3.70$ eV (335 nm) and 5.50 eV (225 nm) (curves 1 and 2, respectively) and at energies of 6.9 and 7.1 eV in the region of the maxima of excitation of the luminescence of excitons localized near Ce^{3+} ions and $\text{Lu}_{\text{Al}}^{3+}$ ADs (curves 3 and 4, respectively). The luminescence decay curve for Ce^{3+} ions excited in the band at 3.7 eV (the $5d^1(t_{2g}) \rightarrow 4f^2(F_{5/2, 7/2})$ transitions) is closest to the exponential dependence with $\tau = 50.7$ ns (Fig. 5a, curve 1). At the same time, upon excitation of the luminescence of Ce^{3+} ions by synchrotron radiation with energies of 6.9 eV (180 nm) and 7.07 eV (175 nm), the luminescence decay kinetics of LuAG:Ce single crystals (curves 3, 4) demonstrates a significant contribution (13.5–35.5% of the initial amplitude) of the slow components with the duration $\tau = 220$ – 280 ns, which are related to the radiative annihilation of excitons at $\text{Lu}_{\text{Al}}^{3+}$ ADs with subsequent excitation energy transfer to Ce^{3+} ions.

In the room temperature range, due to the enhancement of the AD luminescence, the contribution of the slow components to the luminescence kinetics of Ce^{3+} ions in LuAG:Ce single crystals becomes even more pronounced (Fig. 5b). Upon excitation in the band at 6.88 eV (180 nm), which corresponds to the maximum of excitation of the luminescence of the excitons localized near activator ions, the luminescence decay kinetics of Ce^{3+} ions (Fig. 5b, curve 2) is fairly close to the decay kinetics upon excitation in the $4f$ – $5d$ band of Ce^{3+} ions with $h\nu_{\text{max}} = 5.14$ eV (225 nm) (curve 1). At the same time, upon excitation by synchrotron radiation with an energy of 7.74 eV in the onset region of interband transitions in LuAG, the decay kinetics of the luminescence of Ce^{3+} ions becomes much slower (Fig. 5b, curve 3). The expansion of this decay curve in elementary components $I(t) = 152 + 400\exp[-t/(62.5 \text{ ns})] + 905\exp[-t/(288 \text{ ns})]$ indicates a significant increase in the contribution of the slow components with $\tau = 288$ ns to the scintillation amplitude. The corresponding calculation of the contributions of the fast component, which is due to the luminescence of Ce^{3+} ions with $\tau = 62.5$ ns, and the component with $\tau = 288$ ns to the total light sum of LuAG:Ce single crystals showed that the contribution of the slow components ($[I_s/I(t)] \times 100\%$) to the luminescence of LuAG:Ce single crystals is almost 78% at an excitation energy of 7.74 eV (Fig. 5b, curve 3).

The presence of such components is due to the strong absorption of the AD luminescence in the band

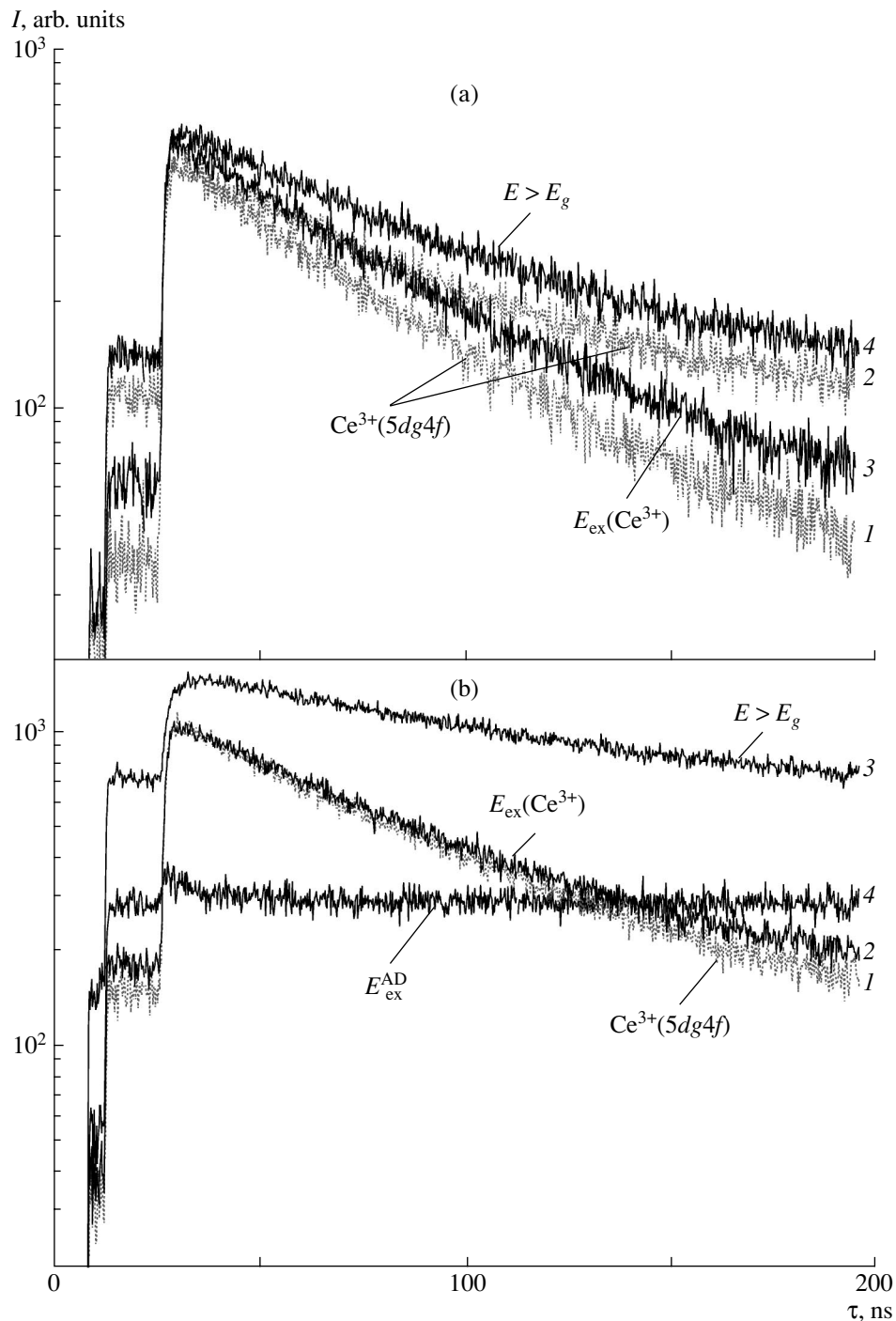


Fig. 5. Luminescence decay kinetics of Ce^{3+} ions in the band with $\lambda_{\text{max}} = 515$ nm in LuAG:Ce single crystals at (a) 9 and (b) 300 K upon excitation by synchrotron radiation with energies of (1) 3.7, (2) 5.5, (3) 6.9, (4) (a) 7.1, and (3) (b) 7.8 eV. Curve 4 in Fig. 5b shows the decay kinetics of the luminescence of $\text{Lu}_{\text{Al}}^{3+}$ ADs in the band with $\lambda_{\text{max}} = 325$ nm upon excitation by synchrotron radiation at a wavelength of 175 nm (7.07 eV).

with $\lambda_{\text{max}} = 325$ nm with the decay time of the main component $\lambda = 538$ ns (Fig. 5b, curve 4) in the $4f-5d$ absorption band of Ce^{3+} ions. Due to this phenomenon, the AD luminescence band becomes as if divided into two bands with $\lambda_{\text{max}} = 318$ and 375 nm. As a result, slow ($\tau = 288$ ns) components caused by this mechanism of

excitation energy transfer arise in the luminescence of Ce^{3+} ions in the band at 2.4 eV (Fig. 5b, curve 3). Thus, in LuAG:Ce single crystals, a peculiar sensitization of the luminescence of Ce^{3+} ions by UV radiation of the centers related to $\text{Lu}_{\text{Al}}^{3+}$ ADs occurs. The second reason for the occurrence of slow components in the lumines-

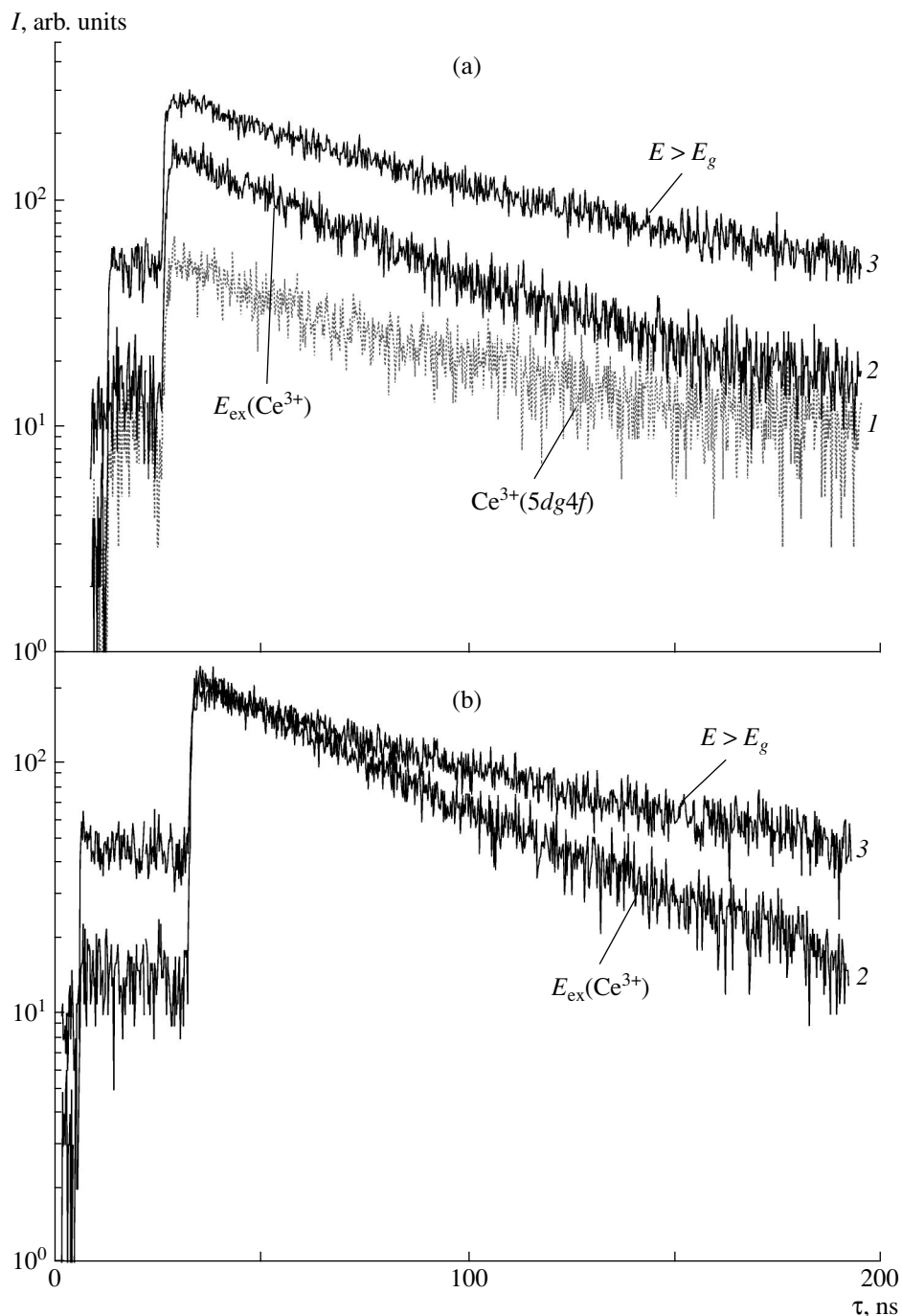


Fig. 6. Luminescence decay kinetics of Ce^{3+} ions in the band with $\lambda = 515$ nm in LuAG:Ce single-crystal films at (a) 9 and (b) 300 K upon excitation by synchrotron radiation with energies of (1) 5.4, (2 (a)) 6.9, (2 (b)) 7.28, and (3) 17.2 eV.

cence of LuAG:Ce single crystals is the intermediate localization of charge carriers at Al^{3+} ADs and vacancy-type defects.

In contrast to LuAG:Ce single crystals, the luminescence decay kinetics in LuAG:Ce single-crystal films at 9 (Fig. 6a) and 300 K (Fig. 6b) upon excitation by synchrotron radiation with energies both in the exciton absorption region ($E = 6.9\text{--}7.3$ eV, curve 2) and in the region of interband transitions ($E = 17.2$ eV, curve 3) is

determined only by the processes of excitation energy transfer to Ce^{3+} ions through the exciton and recombination mechanisms in the absence of components due to the presence of $\text{Lu}_{\text{Al}}^{3+}$ ADs. Upon excitation with an energy of 7.28 eV at 300 K in the exciton absorption maximum (Fig. 4b, curve 4), the component with $\tau = 48.2$ ns is dominant (the contribution to the scintillation amplitude is 94.1%) in the decay kinetics. This component corresponds to the intracenter $5d^1 \rightarrow 4f$ transi-

tions in Ce^{3+} ions (Fig. 6b, curve 3). The presence of a weak (5.9%) slower component with $\tau = 246$ ns at 300 K reflects the real process of excitation energy transfer by excitons to Ce^{3+} ions with subsequent luminescence in the band with $\lambda = 515$ nm. It is not inconceivable that this slow component is due to the presence of two radiative states of excitons localized near Ce^{3+} ions with significantly different transition probabilities. It should be noted that these considerations are also valid for the decay kinetics of the luminescence of Lu^{3+} ADs in the band with $\lambda_{\text{max}} = 320$ nm (Fig. 5a, curve 4) upon excitation at a wavelength of 175 nm at 300 K. The presence of the fast ($\tau = 1.2$ ns) and slow ($\tau = 538$ ns) main components indicates the formation of the AD-related exciton, which is characterized by two radiative levels with different transition probabilities.

In the case of excitation of the luminescence of Ce^{3+} ions in the region of interband transitions ($E = 17.2$ eV), the retardation of the decay kinetics (Figs. 6a, 6b, curves 3), in comparison with the kinetics for the case of excitation of excitons bound by the activator (curve 2), reflects the real time of migration of free electrons and holes to Ce^{3+} ions in LuAG:Ce single-crystal films. For example, the expansion of the decay curve (Fig. 6b, curve 3) in components $I = 8.7 + 99.1 \exp[-t/(50.3 \text{ ns})] + 91.6 \exp[-t/(158 \text{ ns})]$ indicates comparable intensities of the fast and slow components corresponding to the radiative (the $5d \rightarrow 4f^1$ transitions in Ce^{3+} ions) and the migration stages of excitation of this luminescence.

At the same time, the decay kinetics of the luminescence of Ce^{3+} ions in LuAG:Ce single-crystal films both at 9 K (Fig. 6a) and at 300 K (Fig. 6b) is much faster than in LuAG:Ce single crystals. Indeed, in the case of films, there are no slow components that are due to the presence of $\text{Lu}_{\text{Al}}^{3+}$ ADs. In comparison with LuAG:Ce single crystals, the relative contribution of the slow components to the scintillation amplitude for LuAG:Ce single-crystal films is smaller by a factor of more than 3.5: $[I_s/I(t)] \times 100\% = 20.8\%$ (Fig. 6b, curve 3). Thus, LuAG:Ce single-crystal films have much better spectral, kinetic, and scintillation properties in comparison with LuAG:Ce single crystals. Hence, these films can be used for radiation monitoring of α and β particles [6, 13] and visualization of x-ray images [5, 6].

The case of the decay kinetics upon excitation of the luminescence of Ce^{3+} ions in the bands with $\lambda_{\text{max}} = 213\text{--}225$ nm (5.5–5.8 eV), corresponding to the $4f^2(F_{5/2}) \rightarrow 5d^1(2e)$ transitions (the two highest levels of the $5d^1$ shell in the absorption by Ce^{3+} ions) requires special consideration. The decay kinetics of the luminescence of Ce^{3+} ions both in single crystals (Fig. 5a, curve 2) and in single-crystal films (Fig. 6a, curve 1) becomes in this case much slower and differs significantly from that corresponding to excitation in the absorption bands of Ce^{3+} ions in the longer wavelength spectral region, for example, in the band with $E = 3.7$ eV (Fig. 5a, curve 1). This effect was observed previously in the luminescence decay kinetics of YAG:Ce

single crystals [15] and was explained by the fact that the $2e$ levels of the $5d^1$ shell of Ce^{3+} ions are located fairly close to the bottom of the conduction band. As a result, the probability of thermally activated transitions between these levels in Ce^{3+} ions and the levels of the conduction band increases. Hence, the excitation of the luminescence of Ce^{3+} ions is retarded significantly. We believe this effect also occurs in the luminescence of LuAG:Ce single crystals and single-crystal films.

ACKNOWLEDGMENTS

We are grateful to G. Zimmerer for his help in carrying out the experiments at HASYLAB, DESY (Germany). This work was supported by INTAS (project no. 04-78-7083).

REFERENCES

1. M. Nikl, E. Mihokova, and J. A. Mares, *Phys. Status Solidi A* **181**, R10 (2000).
2. J. A. Mares, A. Beitlerova, M. Nikl, *et al.*, *Radiat. Meas.* (2004) (in press).
3. A. Koch, F. Peyrin, P. Heurtier, *et al.*, *Proc. SPIE* **3659**, 170 (1999).
4. A. Koch *et al.*, in *Proceedings of the Fifth International Conference on Inorganic Scintillators and Their Applications, SCINT 99. Moscow, Russia, 1999*, Ed. by V. Mikhailin (Moscow State Univ., Moscow, 2000), p. 157.
5. Yu. Zorenko, V. Gorbenko, I. Konstankevych, *et al.*, *Nucl. Instrum. Methods Phys. Res. A* **486**, 309 (2002).
6. Yu. V. Zorenko, I. V. Konstankevich, V. I. Gorbenko, and P. I. Yurchishin, *Zh. Prikl. Spektrosk.* **69** (5), 665 (2002).
7. Yu. V. Zorenko, A. S. Voloshinovskii, I. Konstankevich, *et al.*, *Radiat. Meas.* (2004).
8. Yu. V. Zorenko, I. V. Konstankevich, V. V. Mikhaïlin, *et al.*, *Opt. Spektrosk.* **96** (2), 280 (2004) [*Opt. Spectrosc.* **96** (3), 390 (2004)].
9. M. Kh. Ashurov, Yu. K. Voron'ko, V. V. Osiko, *et al.*, in *Spectroscopy of Crystals* (Moscow, 1978), p. 7 [in Russian].
10. Yu. V. Zorenko, I. V. Nazar, L. N. Limarenko, and M. V. Pashkovskii, *Opt. Spektrosk.* **80** (6), 925 (1996) [*Opt. Spectrosc.* **80** (6), 832 (1996)].
11. Yu. V. Zorenko, A. S. Voloshinovskii, G. M. Striganyuk, and I. V. Konstankevich, *Opt. Spektrosk.* **96** (1), 78 (2004) [*Opt. Spectrosc.* **96** (1), 70 (2004)].
12. Yu. V. Zorenko, *Opt. Spektrosk.* **84** (5), 856 (1998) [*Opt. Spectrosc.* **84** (6), 856 (1998)].
13. Yu. Zorenko, V. Gorbenko, I. Kostankevych, *et al.*, in *Proceedings of 7th International Conference on Inorganic Scintillators and Their Applications, Valencia, Spain, 2004* (Valencia, 2004), pp. 22–23.
14. E. D. Aluker, D. Yu. Lusic, and S. A. Chernov, *Electron Excitations and Radioluminescence in Alkali Metals* (Zinatne, Riga, 1979).
15. D. J. Robbins, B. Cockayne, B. Lent, and J. L. Glasper, *J. Electrochem. Soc.* **126** (9), 1556 (1979).
16. E. Zych, C. Brecher, and Z. Glodo, *Phys. Condens. Mater.* **12**, 1947 (2000).

Translated by Yu. Sin'kov